International Journal of Computer Science and Application
IJCSA Volume 1, Issue 1, August 2012 PP. 12-18
ISSN(online)
ISSN(print)
www.ij-csa.org

Solution of One-dimensional Hyperbolic Problems Using Cubic B-Splines Collocation

Christopher G. Provatidis[1], Stelios K. Isidorou[2]
[1,2] Department of Mechanical Engineering, National Technical University of Athens, Athens, Greece
Email: [1] cprovat@central.ntua.gr, [2] isidorou_st@yahoo.gr

(Abstract) In this paper we extend the cubic B-splines collocation method to enable it to solve one-dimensional hyperbolic (eigenvalue and wave propagation) problems under arbitrary boundary conditions. This is achieved by analogy with the finite element method, introducing a 'collocation mass matrix' that cooperates with the previously known system matrix, now called 'collocation stiffness matrix'. In agreement with earlier findings on elliptic problems, we found that in time-dependent problems it is again sufficient to use double internal knots (C^1-continuity) in conjunction with two collocation points between successive breakpoints. In this way, the number of unknowns becomes equal to the number of equations, which is twice the number of breakpoints. We paid particular attention to the handling of Neumann-type boundary conditions, where we found it necessary to properly eliminate a column in both mass and stiffness matrices. For the first time, we found that the cubic B-splines collocation procedure (with C^1-continuity) leads to identical results with those obtained using piecewise Hermite collocation. The numerical examples show an excellent quality of the numerical solution, which is far superior to that of the conventional finite element method, for the same number of nodal points.

Keywords: B-splines; Collocation; Eigenvalues; Hermite Polynomials; MATLAB™; Transient Analysis.

1. INTRODUCTION

In the framework of global interpolation methods based on Lagrange polynomials, it has been recently shown that the computation effort may be substantially reduced when applying the collocation instead of the Galerkin-Ritz formulation [1]. However, using spline curves, or piecewise polynomials, is more effective in representing the solution to the differential equation than pure polynomials [2]. The volume of Ascher et al. [3] provides a treatise on spline bases, collocation theory, and spline collocation for application to the numerical solution of boundary-value-problem (BVP) for ordinary differential equations (ODE). Fairweather and Meade [4] give an extensive review (273 papers covering the period 1934–1989) of collocation methods and various implementations. They describe the most common forms of collocation, including nodal, orthogonal, and collocation/Galerkin. An early work towards the solution of eigenvalue problems, however based on Schoenberg's formulation [5], is [6].

In spite of the abovementioned work, so far most part of the relevant research focuses on mathematical topics and reduces mainly to elliptic problems. For example, the FORTRAN codes of [2] have been implemented also in the MATLAB software (formerly under the name *splines tool*) [7], but they operate 'as is' for the solution of linear and nonlinear elliptic problems only. This happens because (i) the eigenvalue and transient analysis require the construction of mass and stiffness collocation matrices, and (ii) although the implementation of Dirichlet type boundary conditions is a trivial task, the same does not hold for Neumann-type ones that require a special treatment. As for the state-of-the-art, the implementation of the function 'spcol' in time-dependent analysis has been made in very few biometrics [8] and chemical engineering applications [9].

In this context, the primary aim of this paper is to investigate the applicability and performance of deBoor's methodology [2] in the numerical solution of hyperbolic problems (eigenvalue and transient). The main novel feature of this work is the development of *mass* and *stiffness* collocation matrices analogous to the finite element method. Consequently, standard eigenvalue analysis based on the QR algorithm, and standard time-integration techniques such as the central difference method will be applied.

In addition to the abovementioned *global* cubic B-splines collocation, *piecewise*-Hermite polynomials (without upwind features) that act between adjacent breakpoints [10] will be compared for the first time. The finding of coincidence is the secondary novel feature of this work.

The theory is sustained by four one-dimensional numerical examples from the field of applied mechanics.

2. FORMULATION

Below is the formulation of typical static (thermal) and dynamic problems and then follows the global B-spline and piecewise Hermite interpolation.

2.1 Thermal Analysis

The steady-state thermal behavior of structures follows Laplace equation. In the particular case of a radially symmetric structure the PDE degenerates to a simple ODE in terms of the radius *r* as follows:

$$\frac{\partial^2 u}{\partial r^2}+\frac{1}{r}\frac{\partial u}{\partial r}=0 \qquad (1)$$

2.2 Elastodynamics – Wave equation

The vibration of an elastic rod is described through the usual hyperbolic differential equation:

$$\frac{\partial}{\partial x}\left(EA\frac{\partial u}{\partial x}\right)+f_x=\rho A\frac{\partial^2 u}{\partial t^2} \qquad (2)$$

where E and ρ denote the material properties, i.e. the Young's modulus and the mass density, respectively, and A denotes the cross sectional area of the rod. Finally, f_x denotes the distributed load along the longitudinal *x*-axis, while *t* denotes the time. In dynamic analysis, the axial displacement, *u*, is a function of both space and time (i.e. $u=u(x,t)$), while in static analysis it is only a function of space (i.e. $u=u(x)$).

Introducing the velocity of the longitudinal elastic wave:

$$c=\sqrt{E/\rho}\,, \qquad (3)$$

in the absence of body forces ($f_x=0$), **Eq.2** receives the well known form of an acoustic wave:

$$\left(1/c^2\right)\cdot\partial^2 u/\partial t^2-\partial^2 u/\partial x^2=0\,. \qquad (4)$$

It is well known that, besides elastic waves, **Eq.4** can also describe wave propagation within acoustic pipes of constant cross-sectional area; in such a case the variable *u* corresponds to the acoustic pressure.

2.3 B-splines Interpolation

B-splines interpolation can be found in many textbooks [2,11], in which efficient procedures to determine the involved basis functions, $N_{i,p}(x)$, can be found. In general, the interpolation within an interval $0\le x\le L$ is given by:

$$u(x)=\sum_{i=1}^{n}N_{i,p}(x)\cdot a_i,\quad i=1,\ldots,n \qquad (5)$$

Concerning **Eq.5**, it should become clear that:

The starting point for the construction of the functional set, $N_{i,p}$, is the selection of the breakpoints and the piecewise polynomial degree, *p*. Let us assume *m* breakpoints, which obviously define (*m*-1) segments. In the sequence, let the polynomial degree be *p* = 3 (cubic B-splines).

(i) The variables a_i involved in **Eq.5** are not directly associated to nodal values (those at the breakpoints), except of those two corresponding to the end points.

(ii) The value of '*n*' depends on the multiplicity chosen for the internal nodes. In this paper, we require C^1*-continuity*, thus the multiplicity must be equal to *two*; therefore, '*n*' is twice the number of breakpoints ($n=2m$). In general, the spline curve is C^{p-1}-continuous everywhere except at the location of the repeated knots where it is C^{p-2}-continuous.

(iii) Therefore, if we choose two collocation points within any of the aforementioned (*m*-1) segments defined by the breakpoints, we can obtain so many equations as the number of the unknown coefficients. In case of elliptic problems, the best choice was found to be two Gauss points at the well-known relative positions ($\xi=\pm 1/\sqrt{3}$), as also was found by deBoor and Swartz [12] (in elliptic problems).

Typical plots of basis-functions are shown in **Figure 1**, in which double knots have been considered. It is noted that both the first and the last basis functions correspond to the left-end and the right-end axial displacement, respectively; these are also a mirror of each other with respect to the center of the interval [0,*L*], and equal to unity at the two ends.

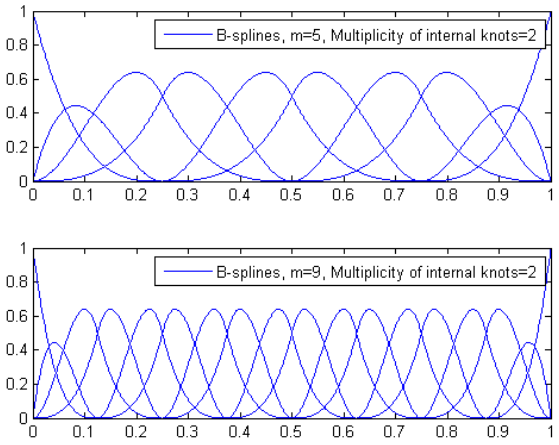

Figure 1. Basis functions in the domain [0,1]. In the top and the bottom there are four subintervals (*m* = 5) and eight subintervals (*m* = 9), respectively; in both cases the internal breakpoints are considered with multiplicity of internal knots equal to *two*.

2.4 Piecewise-Hermite Interpolation

The domain is again uniformly divided into (*m*-1) segments using *m* nodal points (the ends are included). Starting from left to the right, the nodes are numbered by ascending order, whereas the 2*m* degrees of freedom are as follows: $(u_1,q_1),(u_2,q_2),\ldots,(u_m,q_m)$ with $q_i=\left(\partial u/\partial x\right)_{x=x_i}$. In this way, having considered the flux as an independent DOF, C^1-continuity is ensured.

Between any of the (*m*-1) segments, in local numbering the variable *u* is approximated by:

$$u(x,t) = N_1(x)u_1(t) + N_2(x)q_1(t) + N_3(x)u_2(t) + N_4(x)q_2(t) \quad (6)$$

where the shape functions are the well-known Hermite polynomials (**Figure 2**), which are expressed in terms of the normalized coordinate $w = (x/L)$:

$$\begin{aligned} N_1(w) &= 1 - 3w^2 + 2w^3 = 1 - 3\left(\frac{x}{L}\right)^2 + 2\left(\frac{x}{L}\right)^3 \\ N_2(w) &= w - 2w^2 + w^3 = \left[\left(\frac{x}{L}\right) - 2\left(\frac{x}{L}\right)^2 + \left(\frac{x}{L}\right)^3\right]L \\ N_3(w) &= 3w^2 - 2w^3 = 3\left(\frac{x}{L}\right)^2 - 2\left(\frac{x}{L}\right)^3 \\ N_4(w) &= -w^2 + w^3 = \left[-\left(\frac{x}{L}\right)^2 + \left(\frac{x}{L}\right)^3\right]L \end{aligned} \quad (7)$$

It is noted that the above notation presumes that the fluxes q_1 and q_2 are both positive when directed to the positive *x*-axis. Then q_1 causes 'compression' while q_2 causes 'tension'; also the corresponding shape functions in **Figure 2** become anti-symmetric with respect to the middle of the interval [0,*L*] and obtain positive and negative values, respectively. If the convention for q_2 changes, both shape functions may become positive and symmetric with respect to the middle of the domain. Then, the 'mirror' property is obtained for both translational (u_1, u_2) and rotational (q_1, q_2) degrees of freedom.

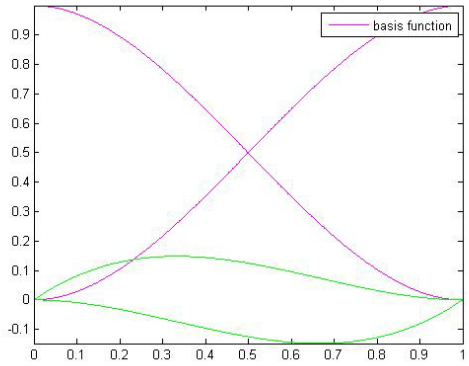

Figure 2. Hermite polynomials defined in [0,1] (blue: translational DOF (N_1,N_3), green: rotational DOF (N_2,N_4)).

3. COMPUTATIONAL PROCEDURE

In all cases below, the ODE is collocated at the $n = 2m$ Gauss points in the interior of the subintervals, i.e. at the locations:

$$x_{col} = \frac{(x_i + x_{i+1})}{2} \pm \frac{1}{\sqrt{3}} \cdot \frac{(x_i - x_{i+1})}{2}, \quad i = 1,\ldots,(m-1) \quad (8)$$

Below, the computational procedure for dealing with eigenvalue and wave propagation problems is presented.

3.1 Eigenvalue Problem

Collocating **Eq.4** at the abovementioned $n = 2m$ Gauss points one obtains the well known matrix formulation [1]:

$$[\mathbf{M}]\{\ddot{\mathbf{a}}(t)\} + [\mathbf{K}]\{\mathbf{a}(t)\} = \{\mathbf{f}(t)\} \quad (9)$$

where $[\mathbf{M}]$ and $[\mathbf{K}]$, both of dimensions $(n-2)\times n \equiv 2(m-1)\times 2m$, are the nonsymmetric mass and stiffness collocation matrices, respectively, which are given by:

$$\begin{aligned} m_{ij} &= \left(\frac{1}{c^2}\right)N_j(x_i), \\ k_{ij} &= -N_j''(x_i), \quad i = 1,\ldots,2(m-1), \quad j = 1,\ldots,2m \end{aligned}, \quad (10)$$

with $N_i(x)$ denoting the shape functions (in global numbering) at the collocation point x_i, in ascending order from left to the right.

It is remarkable that **Eq.9** covers both cases, i.e. the global B-splines interpolation (cf. **Eq.5**) as well as the piecewise Hermite interpolation (cf. **Eq.6** and **Eq.7**).

Concerning the eigenvalue (free vibration) problem, the force vector $\{\mathbf{f}(t)\}$ is taken equal to zero and, therefore, the eigenvalues are extracted by requiring:

$$\det\left\|[\mathbf{K}] - \omega^2[\mathbf{M}]\right\| = 0 \quad (11)$$

In this study we used the standard MATLAB function 'eig'.

3.2 Wave Propagation Problem

The wave propagation problem can be generally solved using either modal analysis or one of the well known time-integration methods (explicit, implicit). In this paper we choose the *central difference* method [13]:

$$\ddot{u}_n = \frac{1}{\Delta t^2}(u_{n-1} - 2u_n + u_{n+1}) \text{ and } \dot{u}_n = \frac{1}{2\Delta t}(u_{n+1} - u_{n-1}). \quad (12)$$

Substituting **Eq.12** into **Eq.9**, the last written for $t_{n+1} = t_n + \Delta t$, one obtains:

$$\left(\frac{1}{\Delta t^2}\mathbf{M}\right)\mathbf{u}_{n+1} = \mathbf{f}_n - \left(\mathbf{K} - \frac{2}{\Delta t^2}\mathbf{M}\right)\mathbf{u}_n - \left(\frac{1}{\Delta t^2}\mathbf{M}\right)\mathbf{u}_{n-1}, \quad (13)$$

from which we can solve for $\mathbf{u}_{n+1}$.

3.3 Boundary Conditions

Despite the apparent simplicity of the procedure, some technical difficulties appear and require special treatment and explanation. First of all, it is reminded that two DOF exist at every nodal point (or breakpoint) for the piecewise cubic Hermite (or B-splines) collocation formulation. Concerning the left and right ends, the DOF correspond to the quantities *u*

and $q=\left(\partial u/\partial x\right)_{x=0 \text{ or } L}$. In every formulation, the vector of the coefficients is as follows (it is reminded that the domain is uniformly divided into (*m*-1) segments using *m* nodal points, where the ends are included):

Piecewise cubic Hermite:

$$\left\{u_1, q_1, u_2, q_2, \ldots, u_{m-1}, q_{m-1}, u_m, q_m\right\}^T$$

Cubic B-splines:

$$\left\{a_1 \equiv u_1, a_2, a_3, a_4, \ldots, a_{2m-3}, a_{2m-2}, a_{2m-1}, a_{2m} \equiv u_m\right\}^T$$

Therefore, for a bar fixed at both ends (or an acoustic pipe open at its both ends), in the piecewise Hermite formulation it is sufficient to eliminate the first ($u_1=0$) and the last minus one ($u_m=0$) columns of the matrices [M] and [K], while in B-splines formulation we must eliminate the first and the last column (it is reminded that B-splines have the "mirror" property).

The situation becomes more complex when dealing with a free end (Neumann-type), for example at *x*=*L*. In this case the strain (or flux, or velocity) is zero or has a given value, but it is *not* always allowed to eliminate the corresponding column. In more details:

(i) In piecewise Hermite formulation the DOF that corresponds to the vanishing flux at the end is quite independent of the rest DOFs, and therefore it can be directly eliminated. In contrast to the FEM analysis, none row is eliminated but only the corresponding columns. Therefore, starting from a matrix system of $\left(n-2\right)\times n \equiv 2\left(m-1\right)\times 2m$ dimensions, the elimination of two DOF leads to a system of $\left(n-2\right)\times\left(n-2\right) \equiv 2\left(m-1\right)\times 2\left(m-1\right)$ dimensions.

(ii) In B-splines formulation the elastic strain (or the acoustic flux/velocity) at the right free end (*x*=*L*) is not an independent variable but it can be derived by taking the first derivative of **Eq.5**:

$$q\left(L\right) \equiv u'\left(L\right) = \sum_{i=1}^{n} N'_{i,p}\left(L\right)\cdot a_i \tag{14a}$$

Due to the compact support of the basis functions, for *p*=3 only the last two out of the *n*=2*m* basis functions have a non-vanishing derivative at *x*=*L*. Therefore, it holds:

$$\begin{aligned} & q\left(L\right) = N'_{n-1}\left(L\right)\cdot a_{n-1} + N'_n\left(L\right)\cdot a_n \\ & \Rightarrow a_{n-1} = \frac{\left[q\left(L\right) - N'_n\left(L\right)\cdot a_n\right]}{N'_{n-1}\left(L\right)} \end{aligned} \tag{14b}$$

For the solution of the eigenvalue problem we can assume that $q\left(L\right)=0$, and therefore **Eq.14b** is somehow simplified. Concerning the matrix term $\left(\left[\mathbf{K}\right]-\omega^2\left[\mathbf{M}\right]\right)\cdot\left\{\mathbf{a}\right\}$, every row can be transformed from its initial form:

$$\begin{aligned} & \left(k_{i1}a_1 + \ldots + k_{i,n-2}a_{n-2} + k_{i,n-1}a_{n-1} + k_{i,n}a_n\right) \\ & -\omega^2\left(m_{i1}a_1 + \ldots + m_{i,n-2}a_{n-2} + m_{i,n-1}a_{n-1} + m_{i,n}a_n\right) \end{aligned} \tag{15}$$

to the final expression:

$$\begin{aligned} & \left[k_{i1}a_1 + \ldots + k_{i,n-2}a_{n-2} + \left(k_{i,n} - N'_n\left(L\right)/N'_{n-1}\left(L\right)\cdot k_{i,n-1}\right)a_n\right] \\ & -\omega^2\left[m_{i1}a_1 + \ldots + m_{i,n-2}a_{n-2} + \left(m_{i,n} - N'_n\left(L\right)/N'_{n-1}\left(L\right)\cdot m_{i,n-1}\right)a_n\right] \end{aligned} \tag{16}$$

Therefore, concerning again B-splines collocation, in case of one Dirichlet boundary condition at *x*=0 and one Neumann condition at *x*=*L*, we proceed as follows. First we eliminate the first column ($a_1=u_1=0$). Then we condense the last two columns in one by subtracting the (*n*-1)-th column (multiplied by the coefficient $N'_n\left(L\right)/N'_{n-1}\left(L\right)$) from the last one. In this way we finally derive a system of $\left(n-2\right)\times\left(n-2\right) \equiv 2\left(m-1\right)\times 2\left(m-1\right)$ dimensions.

Note that the abovementioned condensation is not applicable to the piecewise Hermite formulation, obviously because $N'_3\left(L\right)=0,\ N'_4\left(w\right)=1$.

4. NUMERICAL RESULTS

The performance of the proposed global collocation method will be evaluated in four characteristic test cases: one static (to show the convergence quality) and three dynamic ones. As previously mentioned, from an engineering point of view the dynamic problems may concern either an elastic rod of constant cross-sectional area or, equivalently, an acoustic straight pipe. Since previous studies [12,14] concerning the elliptic problem have shown that the best choice is to use *cubic* B-splines in conjunction with collocation points taken at the two Gauss points between the uniformly distributed breakpoints, results will be presented for these conditions only. For comparison purposes, the collocation method is compared with the conventional finite element (FEM) solution, using the same nodes as the breakpoints.

4.1. Problem 1: Steady-state Conduction in a Cylindrical Wall

This example was chosen because it possesses a non-polynomial (logarithmic) solution. It refers to the potential problem (Laplace equation) with a "steep" temperature distribution, occurring along the radius of a thick long hollow cylinder. The latter is subject to given uniform inner surface temperature (u_1 = 1000 ^{o}C) and a given uniform outer surface temperature (u_2 = 0 ^{o}C) while the inner and outer radii are R_1 = 1m and R_2 = 32m, respectively. The analytical temperature distribution depends on the radial direction only:

$$u\left(r\right) = u_1 + \left(u_2 - u_1\right)/\ln\left(R_2/R_1\right)\cdot\ln\left(r/R_1\right) \tag{17}$$

The radius is divided into a variable number of *n* = 4, 8, 16, 32 and 64 uniform segments. Based on the normalized L_2 error norm ($L_u = L_2\times 100$ in %):

$$L_2 = \sqrt{\int_{R_1}^{R_2} \left(\tilde{u} - u_{exact}\right)^2 dx} \Big/ \sqrt{\int_{R_1}^{R_2} \left(u_{exact}\right)^2 dx}\ , \qquad (18)$$

The excellent quality of the convergence is shown in **Table 1**.

Table 1. Convergence quality of the error norm.

Number of subdivisions (n)	Energy norm L_u (in %)
4	1.19E00
8	0.73E-01
16	0.20E-02
32	2.54E-05
64	1.74E-07

4.2 Problem 2: Elastic Rod Fixed at Both Ends

A rod of length L is fixed at $x = 0$ and $x = L$ and is subject to axial free vibration (equivalently, we could refer to an acoustic pipe with both ends open). The exact eigenvalues are given by:

$$\omega_i^2 = \left(i\pi/L\right)^2 \cdot \left(E/\rho\right),\ i = 1, 2, \ldots \qquad (19)$$

The rod is uniformly divided into 1, 2, 4, 8, 16, 32 and 64 segments. The numerical results are shown in **Figure 3** where one can notice that the convergence is monotonic, of high quality and far superior to the conventional FEM solution.

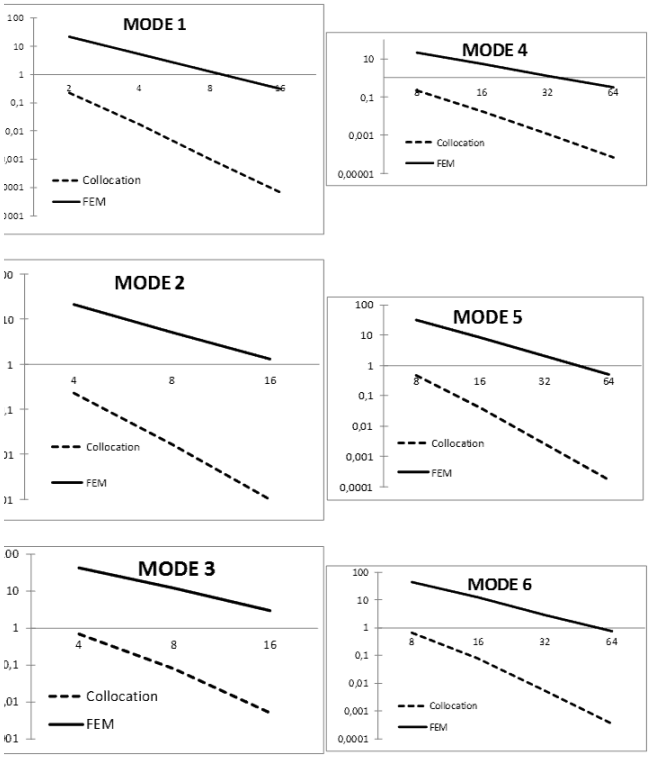

Figure 3. Errors (in %) of the calculated eigenvalues for an elastic rod with fixed ends (the horizontal axis refers to the number n of elements or subintervals of breakpoints).

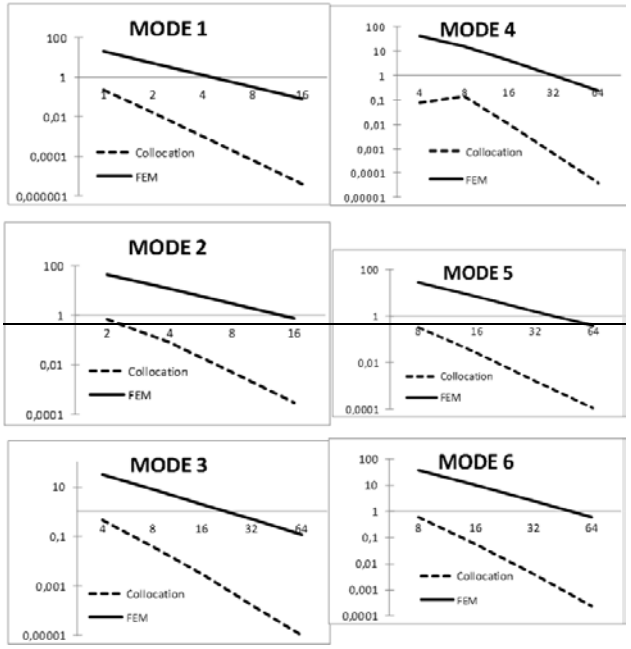

Figure 4. Errors (in %) of the calculated eigenvalues for an elastic rod with fixed left and free right end (the horizontal axis refers to the number n of elements or subintervals of breakpoints).

4.3 Problem 3: Elastic Rod Fixed at Left and Free at Right End

The same rod is now analyzed for different boundary conditions (the equivalent acoustic pipe is open at left and close at right end). The quality of the calculated eigenvalues and the superiority to the FEM is shown in **Figure 4**, where it is expressed as an error (per cent) with respect to the exact solution:

$$\omega_i^2 = \left[\left(2i-1\right)\pi/\left(2L\right)\right]^2 \cdot E/\rho,\ i = 1, 2, \ldots \qquad (20)$$

4.4 Problem 4: Elastic Rod Subjected to a Heaviside Load

An elastic rod of length L is fixed at one of its extremities (x=0) and it is subjected to an axial Heaviside type loading $\sigma_L = Eq_0 H\left(t-0\right)$ [N/m^2] at the other one (x=L). The analytical solution can be found in [15,16]. For simplicity, all geometric and material data were assigned the unitary value. The (explicit) central difference scheme was applied.

For the case of n=8 uniform intervals ($c = \sqrt{E/\rho}$ =1m/s), where the distance between two successive nodes equals to Δx = 0.125m, a very upper limit for the time step could be $\Delta \hat{t}_{cr} = 0.125$ (CFL-criterion). However, for the sake of conservatism, the time step has been conservatively chosen equal to $\Delta t = 0.02\,\Delta x/c$ =0.0025 s. The time history (6000 steps) of the normalized axial displacement at the free end

(x=L) and the middle point (x=L/2) is shown in **Figure 5** and is of excellent quality.

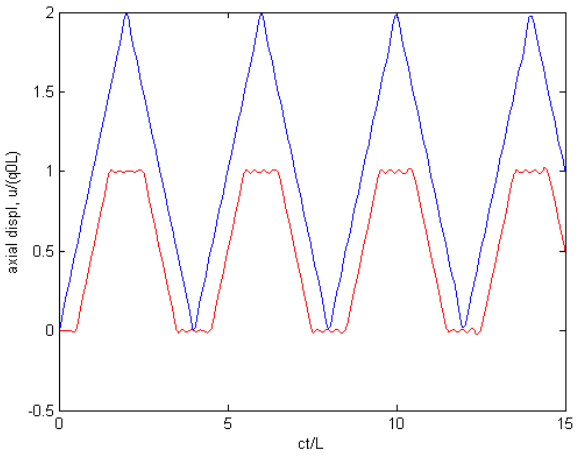

Figure 5. Axial displacement at the free end (x=L) [blue line] and the middle [red line], using the proposed collocation method n = 8 uniform intervals and time step $\Delta t = 0.2\,\Delta x/c = 0.0025$ s

5. DISCUSSION

Similar to previous findings that were obtained for polynomials [1], the superiority of the proposed collocation method to that of the finite element method is due to its global character and the relatively high degree of the piecewise polynomials (p = 3). Clearly, the cubic B-splines interpolation is very smooth and can accurately approximate the involved eigenvectors, while the conventional finite element method uses piecewise linear (hat) shape functions that appear sharp edges at their interfaces (they posses only C^0-continuity).

In all elliptic and hyperbolic numerical examples of this study we found that the cubic B-splines collocation method leads to identical results with those obtained using the piecewise cubic Hermite collocation method. This numerical finding can be theoretically explained as follows. Since two knots are associated to each breakpoint (multiplicity equal to two) it implies that the splines curve is generally C^{p-2}-continuous, where p is the degree of the piecewise polynomial. But as in this study the polynomial degree was chosen to be cubic ($p=3$), the splines curve is C^1-continuous, a fact that is consistent with the C^1-continuity involved in piecewise Hermite approximation (also of third degree).

Although in this type of problems the proposed B-splines interpolation is identical (as for the quality of the obtained results) with the piecewise cubic Hermite collocation method, the first is the vehicle to choose any multiplicity for the internal knots. For example, although no relevant results were reported in this study, we could alternatively choose the multiplicity be equal to *one*, instead of two. In such a case the numerical solution would be C^2–continuous, as it would include a full cubic polynomial plus some Schoenberg's truncated cubic monomials [5]. For example, if we divide the domain [0,L] into four segments, cubic B-splines approximation would lead to seven control points and seven associated coefficients, a_i, $i=1,\ldots,7$. However, since we deal with a two-point BVP, we have to determine only five out of the seven aforementioned coefficients. To this purpose one must choose at least five collocation points within the domain of length L. Obviously, one could use even more than five collocation points but then, since the number of equations would be larger than the number of variables, a least-squares scheme had to be applied. In the same example, although a choice of five (or more, in combination with the least-squares method) Gauss points or Chebyshev roots generally works, the quality of results becomes questionable while the DeBoor's approach (double knots, and two collocation points between successive breakpoints) is always mathematically robust [12].

6. CONCLUSIONS

In this study we achieved to extend the well-known cubic B-splines collocation method, previously used in the solution of elliptic problems only, to one-dimensional hyperbolic ones under arbitrary (Dirichlet of Neumann) boundary conditions. The key point was that, in addition to the system matrix, we achieved to create a mass collocation matrix; thus the computational problem was formulated very similarly to the well known finite element method. Consequently, the eigenvalues were calculated in an algebraic way using standard QR algorithms, while wave propagation (time response) was predicted using a simple central-difference scheme for time-integration. The findings of this study show that the proposed technique has an excellent convergence and its overall performance is far superior to the conventional finite element method for the same number of nodal points. Another interesting finding is that, B-splines collocation based on two knots per breakpoint leads to *identical* eigenvalues and time response with those obtained using again the collocation method but in conjunction with piecewise cubic Hermitian polynomials. Although the results of this study reduced to 1D problems only, on-going research has revealed that extension to 2D (quadrilaterals) and 3D (boxlike) time-dependent problems is a straightforward procedure on the basis of tensor products of the involved control points per direction.

REFERENCES

[1] C. G. Provatidis, Free vibration analysis of elastic rods using global collocation, Archive of Applied Mechanics 78, 241–250 (2008)

[2] C. deBoor, The numerical solution of an ordinary differential equation by collocation, in A Practical Guide to Splines, Edited C. deBoor, Revised Edition, Springer-Verlag, New York, (2001) pp.243-262.

[3] U. M. Ascher, R. M. M. Mattheij and R. D. Russell, Numerical Solutions of Boundary Value Problems for Ordinary Differential Equations (2nd edn), SIAM, Philadelphia (1995)

[4] G. Fairweather and D. Meade, Survey of spline collocation methods for the numerical solution of differential equations, in Mathematics for Large Scale Computing, Edited J. C. Diaz, Lecture Notes in Pure Applied Mathematics, Marcel Dekker, New York (1989), vol. 120, pp. 297–341.

[5] I. J. Schoenberg, Contributions to the problem of approximation of equidistant data by analytic functions, Quart. Appl. Math. 4, 45–99 and 112–141 (1946)

[6] J. W. Jerome and R. S. Varga, Generalizations of spline functions and applications to nonlinear boundary value and eigenvalue problems, in Theory and Applications of Spline Functions, Edited T. N. E. Greville, Academic Press, New York (1969), pp.103-155.

[7] C. deBoor, Private e-mail communications, June-August 2007.

[8] M. Hauptmann, J. Wellmann, J. H. Lubin, P. S. Rosenberg and L. Kreienbrock, Analysis of expose-time-response relationships using a spline weight function, Biometrics 56, 1105-1108 (2000).

[9] H. Pedersen and M. Tanoff, Spline collocation method for solving parabolic PDE's with initial discontinuities: Application to mixing with chemical reaction, Computers & Chemical Engineering 6, 197-207 (1982)

[10] W. Sun, Hermite cubic spline collocation methods with upwind features, ANZIAM J. 42 (E), C1379-C1379 (2000).

[11] L. Piegl and W. Tiller, The NURBS Book, 2nd ed., Springer, Berlin (1996)

[12] C. DeBoor and B. Swartz, Collocation at Gaussian points, SIAM J. Numer. Anal. 10, 582-606 (1973)

[13] K.J. Bathe, Finite Element Procedures. Prentice-Hall/Upper Saddle River, New Jersey (1996), pp. 770-774.

[14] C. G. Provatidis and S. K. Isidorou, Comparison of advanced collocation methods for the solution of ordinary differential equations. In: D. Tsahalis (ed.), CD Proceedings 3rd International Conference on Experiments / Process / System modeling / Simulation & Optimization, Athens, 8-11 July, 2009.

[15] L. A. Pipes and L. R. Harvill, Applied Mathematics for Engineers and Physicists, 3rd ed. McGraw-Hill International Book Company, International Student Edition, (1981) pp.494-496.

[16] C. G. Provatidis, Coons-patch macroelements in two-dimensional eigenvalue and scalar wave propagation problems, Computers & Structures 82, 383-395 (2004).